

Origin of the buckling in the $c(2 \times 2)$ -Si/Cu(110) surface alloy

C. Rojas, C. Polop, E. Román, and J. A. Martín-Gago*

Instituto Ciencia de Materiales de Madrid, C.S.I.C., Campus de Cantoblanco, 28049 Madrid, Spain

R. Gunnella

Università di Camerino, Via Madonna delle Carceri, 62032 Camerino (MC), Italy

B. Brena,[†] D. Cocco, and G. Paolucci

Sincrotrone Trieste S.c.p.A., S.S. 14 Km 163.5, in Area Science Park, 34012 Basovizza-Trieste, Italy

(Received 29 May 1997; revised manuscript received 7 October 1997)

The atomic structure of the $c(2 \times 2)$ -Si/Cu(110) interface has been determined by angle scanned photoelectron diffraction at several electron kinetic energies using synchrotron radiation and by quantitative low-energy electron diffraction (LEED) studies. Experimental photoelectron diffraction scans and LEED I/V curves have been compared through r -factor minimization with single and multiple scattering calculations in order to determine an atomic model for the surface termination. Both techniques show that the $c(2 \times 2)$ superstructure is originated by a two-dimensional alloy in which the Si atoms occupy substitutional Cu sites at the surface layer, with a topmost Si layer vertically displaced inward by 0.26 ± 0.04 Å. A possible mechanism for the origin of the corrugation based on a strong chemical bonding between the Si deposited atoms is proposed. [S0163-1829(98)02304-2]

I. INTRODUCTION

In the last decade, the study of the growth of ultrathin films has greatly progressed. Much of the effort on this matter has mainly been devoted to the growth of two-dimensional (2D) layers with properties different from those of the bulk. This is the case for surface alloys. The atomic structure of an ordered surface alloy consists of a single ordered and mixed top atomic plane, where usually one out of two surface atoms are replaced by the deposited atom. Among the recent structurally resolved surface alloys are Au-Cu(100),¹ Pd-Cu(100),² Mn-Cu(100),³ and Mn-Ni(100).⁴ Particularly, in the last few years, unusual magnetic properties have been found in Mn-Cu(100) (Ref. 5) and Mn-Ni(100).⁶ In these cases, a structural low-energy electron diffraction (LEED) analysis showed a highly corrugated surface where the Mn atoms are found to be relaxed outward by 0.3 ± 0.02 Å in MnCu and by 0.25 ± 0.02 Å in the MnNi surface alloy. However, for the nonmagnetic surface alloys, a very slight buckling ($+0.02$ Å) has been observed. Therefore, the phase stability and the corrugation amplitude in these alloys have been attributed to the high spin state of the Mn atoms rather than to the simple atomic size argument (the corrugation increases with the increasing size of the deposited atoms) proposed in Ref. 2. In this work we present a detailed study on the origin of the buckling by studying the corrugation of a type of surface alloy very recently reported.⁷ In the $c(2 \times 2)$ Si-Cu(110) surface structure both atoms have very similar atomic radii and magnetic properties are not present. It will be shown that there is an inward surface relaxation, that cannot be explained by any of the previously considered mechanisms. Therefore, a strong chemical interaction between the surface deposited Si atoms is suggested to be responsible for the vertical corrugation of this alloy.

There is a lack of scientific information about semicon-

ductor deposition on metal surfaces. Most of the structural work performed up to now have been carried out either by depositing Si by adsorption and decomposition of silane^{8,9} or by diffusing it from the bulk.¹⁰ In all this previous work, the formation of Si-metal terminated overlayer is reported.

To gather information about the surface structure of this two-dimensional alloy a combination of x-ray photoelectron diffraction (XPD) and LEED has been used. In spite of the fact that both techniques are well established and currently used, very few studies compare the structural results obtained on the same system by using both of them. These techniques have been previously used for evaluating the buckling of the surface layers.^{12,3} Particularly, both these techniques have been applied to the Mn-Cu(100) case, leading to some differences in the buckling estimation. Thus, an important motivation for the present work is to perform a comparative study of the results obtained by both techniques. In the experiments we present hereafter, LEED I/V and XPD experimental data were recorded one after the other, after each sample preparation. In this way we can rule out differences in the sample preparation. Three different analyses of the experimental data have been performed. XPD photoelectron diffraction scans have been analyzed by single scattering cluster (SSC) and multiple scattering (MS) calculations. In addition, LEED I/V curves have been fitted by using full dynamical calculations. The results obtained for all three analyses agree within their error bars. Also, this work shows a comparative study between the SSC and MS analysis applied to the same system. The XPD structural results drawn from this paper, clarify the real magnitude of the errors and energy range of applicability of the SSC calculation method to determine structural parameters in coplanar systems.

The atomic structure of the $c(2 \times 2)$ -Si/Cu(110) interface has been recently determined with full-hemispherical x-ray photoelectron diffraction⁷ using a x-ray tube. In this work, it

is concluded that the surface atomic structure consists of an almost coplanar layer, where the Si atoms replace one out of two surface Cu atoms. Comparing the experimental data with single scattering cluster calculations via a bidimensional r factor, the Si atoms are found to be around $\Delta z = -0.05 \pm 0.10$ Å below the surface layer. This atomic model is schematically represented in Fig. 1. Hereafter we present a different approach to the structure which consist of measuring XPD azimuthal scans at different photon energies. In agreement with previous work,⁷ we have found that the Si atoms are located in a lower position with respect to the surface Cu atoms. On the other hand, the buckling of the surface layer found in this work is higher (-0.26 ± 0.04 Å) than in the previous work. Although small, the structural difference between both determinations is not within the error bars, and the possible origin for the discrepancy between them is discussed in the text.

Section II describes the experiment and gives details about the calculation procedures. In Sec. III we present the LEED and the XPD analysis and we compare SSC with MS calculations. Section IV is devoted to discuss and to summarize the results.

II. EXPERIMENTAL DETAILS

Experiments were carried out at the SuperESCA beamline at the ELETTRA synchrotron radiation facility.¹² The photon energy was varied between 178 and 800 eV. The end station is an ultrahigh vacuum chamber equipped with an hemispherical electron analyzer, LEED, and a computer assisted sample manipulator. The overall energy resolution (beam line+analyzer) at 178 eV was around 80 meV. Cu(110) samples were prepared by repeated cycles of ion bombardment and annealing to 550 °C. After the cycles the surface exhibited the characteristic 1×1 sharp LEED pattern. XPS confirmed the absence of O, C, and S impurities at the surface prior and after deposition. Si was evaporated *in situ* using an electron bombardment Si cell previously calibrated by a quartz crystal. In addition to that, the coverage was estimated by measuring the Cu3*p* to Si2*p* core levels intensity ratio. In this work, 1 monolayer (ML) is considered to be the number of Cu atoms present on the $[110]$ rows. In these experiments, the $c(2 \times 2)$ structure was produced by deposition of 0.55 ± 0.05 ML. The working pressure was in the low 10^{-8} Pa. Both XPD scans and LEED I/V curves were measured after each sample preparation. In this way differences induced by variations in sample preparation (i.e., coverages, substrate or source temperature, etc.) are avoided. A complete experimental set took around 12 h and after the experiments it was checked by x-ray photoemission spectroscopy (XPS) and LEED that the surface was not contaminated.

All XPD scans presented in this article were performed moving the sample for a fixed photon energy. Polar angles are referred to the surface normal and azimuthal angles to the $[110]$ direction. The angular error in the sample goniometer is less than 1° . XPD data were collecting by measuring the area of the Si2*p* XPS peak. A video LEED system¹² was used to record simultaneously the intensity of ten nonequivalent beams $[(01), (10), (1,1), (2,1), (1,2), (0,2), (2,0), (\frac{1}{2}, \frac{1}{2}), (\frac{3}{2}, \frac{1}{2}), \text{ and } (\frac{1}{2}, \frac{3}{2})]$ in an energy range from 50 to 250 eV with

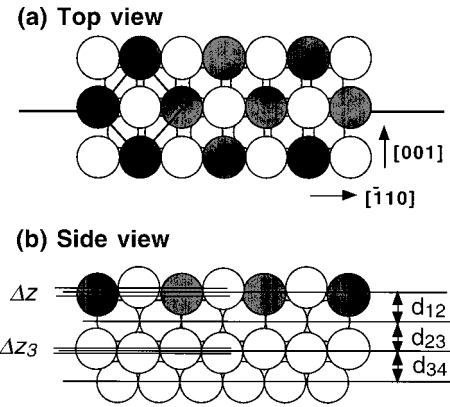


FIG. 1. Schematic structural model for the $c(2 \times 2)$ Si/Cu(110) surface alloy. (a) Top view, (b) side view along the thick line of (a), including the definition of the structural parameters used for the LEED analysis. The surface unit cell of the $c(2 \times 2)$ surface structure is indicated. Filled circles represent Si atoms and empty circles Cu atoms.

normal incidence. The experimental curves were recorded at room temperature and the total data set measured was 1443 eV. Experimental data were corrected for background subtraction.

III. EXPERIMENTAL RESULTS AND DISCUSSION

The surface termination geometry presented in Ref. 7 and derived from the present study is sketched in Fig. 1. This corresponds to a Cu(110) surface where one out of two Cu atoms from the surface rows are replaced by a Si atom (darker circles in the figure). The Si atoms are at a different vertical position with respect to the surface Cu atoms (buckling, Δz). By analyzing angle-scanned XPD data we can obtain accurate information about the buckling of the most external layer Δz . The interlayer distances (d_{12}, d_{23}, d_{3b}) and a buckling in the third layer Δz_3 estimated by the LEED analysis are also shown in Fig. 1.

A. LEED results

The best established and most accepted technique for elucidating surface structures is quantitative LEED analysis. A complete set of LEED I/V curves were recorded from the $c(2 \times 2)$ superstructure. In order to reproduce the measurements, LEED calculations were performed using full dynamical calculations based on modifications of the Huang and Tong code.¹³⁻¹⁵ This formalism uses the muffin-tin approximation to describe the electron scattering by the atomic potentials in the lattice. The interlayer scattering was treated by matrix inversion. The layers were stacked by the layer doubling method. Thermal vibrations were considered by means of a layer dependent Debye-Waller factor Θ_D . The structural search was carried out by two methods: a parameter space scan in a reasonable range and the Levenberg-Marquardt (LM) algorithm using full dynamical formalism.¹⁵⁻¹⁸ We also performed an optimization of the nonstructural parameters. For the quantitative comparison of experiments and theory, the Pendry (R_P) and that defined by Moritz (R_{DE}) r factors¹⁷ have been used. The error bars have

TABLE I. Summary of the structural results derived from this work. See Fig. 1 for definition of the magnitudes. Values are given in Å. $d_b=1.27$ Å.

	Δz (Å)	d_{12} (Å)	d_{23} (Å)	Δz_3 (Å)	d_{3b} (Å)
LEED	-0.24 ± 0.02	1.08 ± 0.03	1.39 ± 0.05	-0.10 ± 0.03	1.24 ± 0.06
XPD-MS	-0.24 ± 0.04				
XPD-SSC	-0.30 ± 0.1				

been deduced after Pendry,¹⁹ from the variance of R_p . More details about the LEED calculation procedure can be found elsewhere.²⁰

The best fit was found at $R_p=0.21$ and $R_{DE}=0.30$ for the structure sketched in Fig. 1 and described in Table I. The real and imaginary part of the optical potential are $V_{0r}=5$ eV and $V_{0i}=5$ eV, respectively. The Debye temperature was fitted to $\Theta_D=422$ K for the bulk Cu atoms, $\Theta_{SD}=372$ K for the Cu atoms of the top layer, and $\Theta_{Dsi}=671$ K for the Si atoms.

The minimum of the r factor (R_p) is similar to other LEED studies in other surfaces alloys (0.28 and 0.31 for Mn-Ni and Mn-Cu, respectively in Ref. 4). Figure 2 shows some selected measured I/V beams with its respective calculation underneath. A visual inspection of these curves shows that both peak position and intensities are fairly well reproduced by the theory as expected from the low r -factor value. Figure 3 shows the Pendry r -factor calculation as a function of the vertical corrugation. A deep minimum is clearly appreciated around $\Delta z = -0.24\pm 0.02$ Å. The error bar in the buckling determination is indicated in Fig. 3 by a horizontal line.

B. Photoelectron diffraction results

As already mentioned, XPD scans were measured from the same sample preparation round as the previously discussed LEED I/V curves. A set of experimental XPD azimuthal scans is shown in Fig. 4 together with its corresponding SSC calculation. The electron kinetic energies are indicated on the left of each scan. The angular dependence of the photoemission intensity is referred to the minimum of the intensity I_m and normalized with respect to the maximum I_M

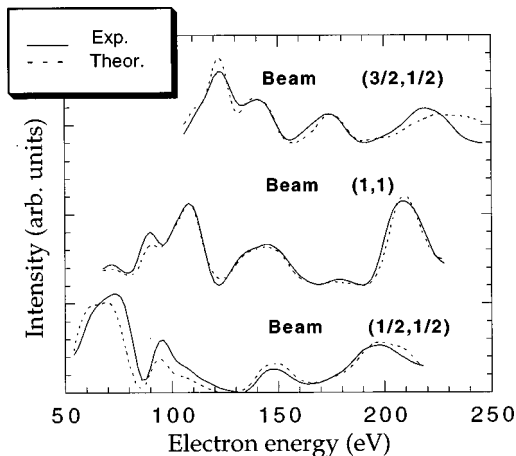


FIG. 2. Experimental LEED I/V curves for the $c(2\times 2)$ Si-Cu(110) (solid line) compared with its best fit calculation (broken line) for some selected beams.

of the photoemission intensity: $\chi=(I-I_m)/I_M$. The experimental points of Fig. 4 have been obtained by integrating the Si2p core level photoemission peaks. The azimuthal scans have been measured at a polar angle of 72° . The choice for this angle was a compromise: higher polar angles strongly reduce the total count rate, and smaller angles lead to a reduction of the high order interference features, resulting in both cases in a decreasing of the experimental anisotropy. The experimental curve recorded at 695 eV of kinetic energy (upper part in Fig. 4) has only been measured around the $[\bar{1}10]$ direction because experimental beam time constraints. However, due to the symmetry of the $c(2\times 2)$ atomic model (Fig. 1) a fit of the structure around this direction also accounts for the atomic positions around the $[001]$ surface direction. It has been verified that the final conclusions do not depend on the angular range considered. In the SSC calculations we have used as parameters to fit and minimize the inner potential V_0 , the electron free mean path λ , and surface and bulk mean square atomic displacement $\langle u^2 \rangle$. Best agreement has been found for 4 V, 3 Å, 0.022 Å², and 0.058 Å², respectively. The structural result obtained from the fit, depends slightly on these parameters (≤ 0.1 Å). The SSC calculated scans based on this proposed model (continuous lines in Fig. 4) reproduce the angular position of most of the experimental fine structure features present in the XPD scans. The little peaks appreciated in the $[\bar{1}10]$ and $[001]$ directions correspond to the tail of the forward scattering emission.⁷ The distance between Si and Cu along the $[\bar{1}10]$ direction causes the first order interference maximum to appear in the position indicated by an arrow in Fig. 4. It can be observed how the arrow position moves away from the forward scattering peak as the kinetic energy is decreased.²¹

In order to give an accurate value for the vertical displacement Δz , a trial and error procedure was performed. To

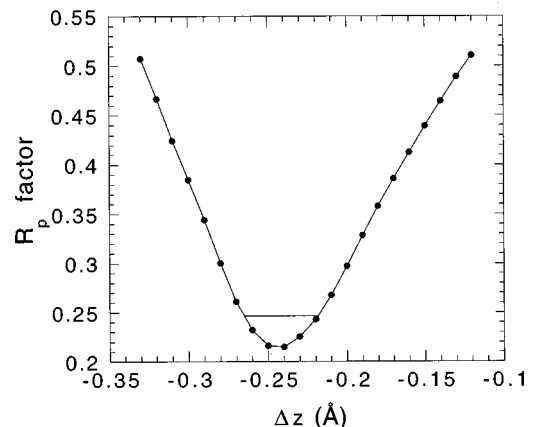


FIG. 3. Pendry r_p -factor curve obtained by comparing the experimental LEED I/V curves with calculations for different distances between the Cu and Si layer, Δz .

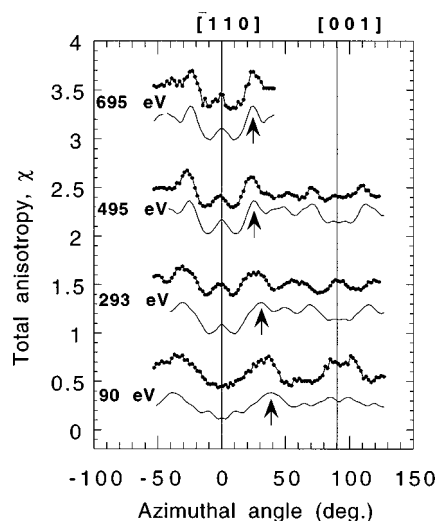


FIG. 4. Photoelectron diffraction azimuthal scans of the Si $2p$ photoemission peak for the Si/Cu(110) surface alloy. The different curves have been recorded at different electron kinetic energies, indicated at the left. Dotted curves are the experimental points and the solid lines underneath represent the single scattering cluster calculation for the best fit structure. The polar emission angle was 72° . Small arrows indicate the calculated position for the first order of interference.

evaluate the quality of the fit two different reliability factor have been used. One based on the Pendry r factor¹⁹ r_p , and another on the standard deviation r_2 factor.²² The r_p factor is more sensitive to the peak positions rather than to absolute intensities. Both r factors lead to the same structural result.

In Fig. 5 the result of applying a Pendry r_p factor to each of the experimental curves of Fig. 4 is presented. The minimum of the curves of Fig. 5 shows the best agreement between the single scattering cluster (SSC) theory and experiments and then, it corresponds to the best determination of the Cu-Si vertical distance (Δz). It can be observed in Fig. 5, that the minimum value for all of the curves appears in a wide Δz region ranging from -0.4 to -0.2 Å (indicated by a straight line in Fig. 5), and therefore it can be stated from a SSC analysis that the Si atoms present a vertical displacement respect the Cu atoms of -0.3 ± 0.1 Å.

The good agreement between theory and experiments indicates that the atomic geometry proposed in the model of Fig. 1 is correct and atomic distances are in this range. Nevertheless, it can be appreciated in Fig. 5 that the minimum of the curves is deeper as the electron kinetic energy increases, indicating a better agreement between theory and experiments. For the higher electron kinetic energy curve of Fig. 5 the r_p -factor minimum appears at around 0.22, a value comparable to the one obtained by the LEED analysis (Fig. 3). Particularly, the r_p -factor curve for 90 eV of kinetic energy shows very small variations for the whole Δz range. As will be discussed later, when the kinetic energy is reduced multiple scattering events become more important and the use of the SSC theory could be inappropriate. Nevertheless it can be appreciated that the main features in the 90 eV spectrum around [110] are fairly well reproduced by the simple SSC code.

To improve the fit for the low kinetic energy region, an independent calculation has been done using a more sophis-

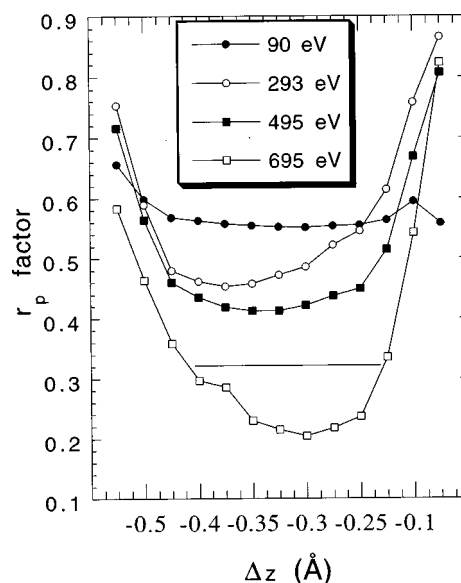


FIG. 5. Pendry r -factor curve obtained by comparing the experimental curves of Fig. 4 with SSC calculations for different distances between the Cu and Si layer Δz .

ticated MS formalism²³ with a complex potential, which has been previously used to study clean²⁴ and adsorbed surfaces.²⁵ In this multiple scattering analysis the cluster size after convergence, assured by the complex phase shifts and k vectors in the mathematical description of propagators, had 156 atoms and 4 planes of scatters. The angular momentum expansion was done up to $l_{max} = 5$. The calculated mean free path was about 5 Å. The value of the interstitial potential varying from 4 to 7 eV does not change the structural result of the minimum search. The minimization procedure was performed by means of a SIMPLEX routine with a Metropolis algorithm for the annealing simulation,¹⁶ recently developed to study the clean Si(001)- 2×1 surface structure.²³ During this minimization, the kinetic energy and the angle (azimuthal for polar scans and polar for azimuthal scans) were free parameters in the calculation, together with the main structural parameters of the surface and the interstitial potential. No linear tensor approximation has been attempted and the full calculation has been redone at each iteration. Due to the little interstitial potential (4–7 eV) the angle which minimizes the structure is not at all affected by the refraction rule.

This formalism has been applied to the XPD scans recorded at lower kinetic energies. A polar scan measured at 78 eV of kinetic energy along the [110] surface direction, together with some calculated scans for different values of the vertical distance between Si and Cu atoms Δz is shown in Fig. 6. The calculation which present the best fit to the experimental data is plotted with a thicker line. As already mentioned, a second r factor (r_2) was also calculated. It is the sum of the absolute values of the difference between a normalized theoretical curve and the experimental one divided by the number of experimental points:

$$r_2 = \frac{\sum_j |\chi_j^{th} - \chi_j^{exp}|}{N}.$$

Figure 7 shows r_2 evaluated for the MS calculation of the azimuthal scan represented in Fig. 4 at 90 eV of kinetic

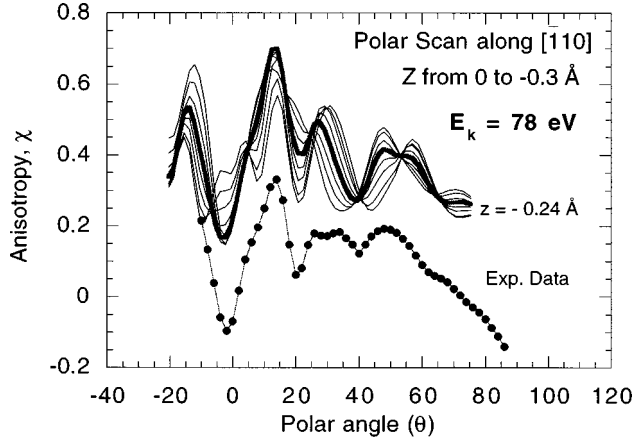


FIG. 6. Experimental photoelectron diffraction polar scan of the $\text{Si}2p$ peak recorded along the $[110]$ surface direction for a kinetic energy of 78 eV (dotted curve). The continuous lines represent different MS calculations varying the distance between the Cu and Si layer, Δz . The best fit to the experimental data is plotted with a thicker line.

energy (full squares symbols in the figure) and of the polar scan along the $[110]$ direction from Fig. 6 (full circles). All the curves present a clear minimum corresponding to $\Delta z = -0.24 \pm 0.04 \text{ \AA}$. A similar result has been obtained by analyzing polar scans along the $[001]$ and $[112]$ surface directions (data not shown for conciseness).

This r factor r_2 was also evaluated for the SSC calculation of the same angular scans and the resulting curves are also shown in Fig. 7 (empty squares and empty circles). The applicability of angle scanned XPD technique for determining coplanar structures is evident after the examination of the Figs. 5 and 7. Recording azimuthal scans at grazing angles, the simple SSC calculation gives good agreement with the

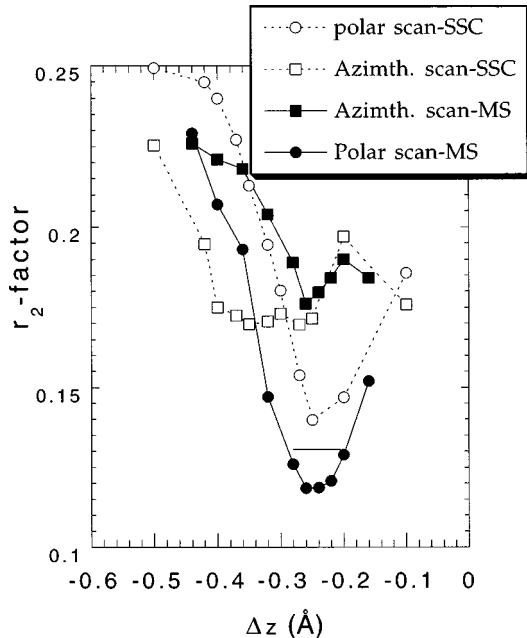


FIG. 7. r_2 -factor curve obtained by comparing several XPD polar (circles) and azimuthal scans (squares) with MS (full symbols) and SSC (empty symbols) calculations for different distances between the Cu and Si layer Δz . See text for r -factor definition.

atomic structure derived from a LEED study. However, the quality of the analysis (as judged by the r factor curves) improve strongly as the kinetic energy is increased (Fig. 5). When angle scanned photoelectron diffraction is performed by recording grazing azimuthal scans the information about the atomic positions comes out from the analysis of the high order interference features.^{21,26} These features are more intense and better defined as the kinetic energy is increased. For low kinetic energies the high order interference features get broader because of the energy dependence of the scattering factor and then, it is difficult to extract the structural information from the azimuthal scans. This fact is manifested in the r -factor curves of Fig. 5: at lower kinetic energy, wider curves with higher r -factor values are obtained. Moreover, at low kinetic energies (around 100 eV) the back-scattering is strong and makes photoelectron diffraction sensitive to the interlayer spacing when the photoemission intensity is measured close to normal emission. This fact is illustrated in Fig. 7. For low kinetic energies grazing azimuthal scans give wide r -factor curves and worse agreement than polar scans. From these curves it is also evident that a MS calculation strongly improves the quality of the fits for the polar scans but not for the azimuthal scans. Nevertheless, it is important to remark that with a simple SSC calculation one can easily get the atomic geometry and distances in the atomic model.

The fact that both SSC and MS analyses found an inward corrugated surface indicates the sensitivity of the XPD technique for evaluating nearly coplanar atomic structures. The 0.06 \AA difference between the MS and the SSC evaluation of Δz is just within the error bar. The SSC theory has probed its validity for evaluating surface structures^{7,27-29} even for kinetic energies as low as 100 eV. Recently, the validity of a SSC approximation for evaluating interlayer spacing of the Ta(100) surface by analyzing low-energy XPD features has been reported.²⁸

IV. DISCUSSION

In the present study we have found that $\Delta z_{\text{SSC}} = -0.30 \pm 0.1 \text{ \AA}$, $\Delta z_{\text{MS}} = -0.24 \pm 0.04 \text{ \AA}$, $\Delta z_{\text{LEED}} = -0.24 \pm 0.02$. These values are in excellent agreement and within the error bars. The whole set of structural values derived from these analyses are summarized in Table I. In this work, the error in the buckling determination has been evaluated by examining the r -factor curves. The position in the r -factor curves where the error bar has been taken is indicated in Figs. 3, 5, and 7 by a horizontal line. For the XPD analysis, these values are slightly higher than the obtained by a classical statistical analysis (i.e., variance). Thus, the final value of Δz can be assumed to be an average of the three results obtained by independent analysis. A very conservative error can be taken to be the intersection of all of them and therefore, a final value for the surface corrugation of $\Delta z = -0.26 \pm 0.04 \text{ \AA}$ can be derived from this work.

In Table II we summarize the main results obtained up to now on different surface alloys for the buckling together with the difference in atomic radii for the deposited and substrate atoms. It can be appreciated that in all cases the deposited atoms have a bigger atomic radii than the substrate atoms, and then an outwards relaxation is expected in all

TABLE II. Summary of the buckling Δz (Å) difference in atomic radii ΔR (Å) and interlayer variation d_{12} (%) for different ordered surface alloys. The references from which the values have been taken are indicated.

	Δz (Å)	ΔR (Å)	Δd_{12} (%)
Au-Cu(100) (Ref. 1)	0.1	0.18	+4.2
Pd-Cu(100) (Ref. 2)	0.02	0.09	+0.7
Mn-Cu(100) (Ref. 4)	0.3	0.07	+7.4
Mn-Cu(100)-XPD (Ref. 9)	0.39	0.07	+0.9
Mn-Ni(100) (Ref. 4)	0.25	0.11	+10.5
Si-Cu(110) (Ref. 7)	-0.05	0.04	-
Si-Cu(110) (this work)	-0.26	0.04	-15 (-5.9%)

cases. However, in the case under study, the detection of forward scattering peaks in the Si2*p* photodiffraction experiments for grazing angles⁷ (see Fig. 2) assure that the Si atoms are located underneath of the Cu surface.

The in-plane atomic structure schematically represented in Fig. 1(a) exhibits some similitudes and differences with the found for others Si/Cu systems.^{8,9} A incommensurated bidimensional overlayer with hexagonal symmetry of Cu₂Si is formed when Si is deposited on Cu(100) via a saturation exposure of Silane.⁹ The Si-Cu distance in the overlayer is 2.46 Å. In our case the first nearest neighbor distance is 2.55 Å, which is imposed by the Cu lattice. The structure proposed for Si/Cu(100) has a remarkable similarity with the Cu/Si(111) (Ref. 30) system. Both works found a locally hexagonal Cu₂Si planar overlayer with very close interatomic distances. Interestingly, we found in the present work that the Si atoms forms a bidimensional overlayer but the stoichiometry of the surface is CuSi, similar to the one found for Si segregated on Si_(1-x)Fe_x(100) (Ref. 10) and other bimetallic surface alloys¹⁻⁶ grown on the (100) face of fcc metals. An accurate determination of the atomic position has not been performed for the semiconductor-on-metal systems referred to earlier.

Up to now, two different mechanisms for the buckling of ordered surface alloys have been proposed. It has been suggested that the corrugation surface alloys increases with increasing differences in atomic diameters of the constituting elements. This is summarized in Table II, where the differences in atomic radii for the studied alloys are shown in the second column. This simple model explains the trend for Au and Pd but it fails for Mn. For this reason, the magnetic interaction as the driven force for the large corrugation has been proposed ulteriorly. However, Si-Cu forms nonmagnetic surface alloys, and then, weak corrugation could be expected from this theory. The change in the sign and large relaxation value found in this work suggest that neither magnetism nor a simple difference in atomic radii are responsible for the buckling and other different mechanism should be invoked to explain its vertical relaxation.

Another striking structural result obtained in this calculation is the unusual large relaxation of the second layer d_{12} [$\Delta d_{12} = (d_{12} - d_b)/d_b \times 100$] [$d_b = 1.27$ Å, for Cu(110)] which is estimated to be around -15% (see Table II). However, if this distance is considered with respect to the Cu topmost plane, the contraction is only of -5.9%. This value is more likely, and it is of the same order of the one found

for the clean Cu(110) surface by LEED studies, -8.5%.^{20,31} This fact suggests that the buckling, although having negative sign, is not strongly affecting the Cu inner layers. Thus, it could be that Si atoms bond parallel to the surface forming a strong covalent bond with the next Si atom of the surface and very weak with the rest of the surrounding Cu atoms. This bonding can lead to an important reduction of the Si radii. Recent STM images have revealed the presence of charge density along the diagonal of the surface unit cell (i.e., the [112] surface direction, see Fig. 1) which could correspond to a Si-Si bonding.³² This charge arrangement leads to an important core level shift for the Si2*p* peak (around 0.5 eV).²⁰ However, it is difficult to discern whether the shift is induced by charge transfer from the neighboring Cu atoms or by final state effects due to the screening of the core hole. Moreover, ultraviolet photoemission (UPS) studies of the valence band modification upon Si coverage have shown that the Cu electronic states are not modified by the surface alloy layer.³³ This fact is also suggesting a Si-Cu overlayer slightly interacting with the Cu inner layers. In the third column of Table II the variations in d_{12} distances with respect to the clean surface for the previous studies are summarized. A big dispersion of the data is observed for this magnitude. The second interlayer spacing is also found to be expanded by 9.0%, whereas in the clean Cu(110) surface is found to expand by 2.3%. For Mn-Cu an unexpected buckling in the second layer instead of in the third layer as required by the symmetry of the system and what we found in this work is observed.⁴

In a previous work on Si-Cu(110) a value of -0.05 ± 0.1 Å was found for the surface relaxation by angle scanned XPD.⁷ Although both results indicate the same trend, i.e., a inwards relaxation, the obtained values are out of the error bar. The result of the buckling obtained in Ref. 7 has been revised by measuring the angular distance from the first order interference fringe to the forward scattering peak. Thus, it has been verified without an extended calculation, that the experimental data indicate the existence of a nearly coplanar Si-Cu overlayer. It is worthy to note that also disagreement in the experimental determination of the buckling in the Mn-Cu(100) system by energy scanned XPD and LEED has been reported.^{3,11} Particularly, in Ref. 11 performing further structural analysis by different techniques is suggested. In this work we found agreement between different experimental techniques performed on the same round of measurements, but disagreement with other different works using the same experimental technique. Thus, the difference between both results cannot be induced by an error in the data analysis, and therefore the difference in the buckling estimation could be originated by the difference in experimental conditions. Since in this work the XPD and the LEED data were recorded one after the other, from the same surface preparation, we conclude that changes in the structural parameters induced by differences in the sample preparation (i.e., substrate temperature, coverage, deposition rate, defects, terrace width, etc.) are not meaningful in the present work and they could be at the origin of the reported differences. Particularly, the measurements of Martin-Gago *et al.*⁷ were performed for a total coverage of 0.4 ML, before the saturation coverage. The work presented here was performed just after the saturation coverage (around 0.55 ± 0.05 ML).

Recent STM images have revealed that there are differences in the surface morphologies for both coverages.³² It could be that the strongly Si-Si bonded layer parallel to the surface plane slightly accommodate its height with respect to the surface Cu plane depending on surface stress, surface defects, steps, and other experimental parameters. Thus, Si would form a nearly floating overlayer, as has been reported to happen for the hexagonal Cu₂Si alloy.⁸

Summarizing, an atomic model for the $c(2\times 2)$ Si/Cu(110) interface has been refined by means of the XPD and LEED techniques. We have found that the topmost mixed layer is relaxed inward by around 0.26 ± 0.04 Å. The origin for this buckling could be a strong chemical bonding be-

tween the neighboring Si deposited atoms (along the $[112]$ surface direction) and very weak interaction with the rest of the coplanar Cu atoms and with the second Cu layer.

ACKNOWLEDGMENTS

We are grateful to J. L. Sacedón for useful discussions and to J. Cerda, W. Weiß, and S. Gallego for computing assistance with the LEED calculation. This work was partially supported by the Spanish CYCIT project PB94/53 and by the European Union under Contract No. ERBCHGECT 920013 (access to large scale installations).

*Author to whom correspondence should be addressed. Electronic address: gago@icmm.csic.es

[†]Present address: Department of Physics, Uppsala University, Box 530, S-751 21 Uppsala, Sweden.

¹Z. Q. Wang, Y. S. Li, C. K. C. Lock, J. Quinn, F. Jona, and P. M. Marcus, *Solid State Commun.* **62**, 181 (1987).

²S. C. Wu, S. H. Lu, Z. Q. Wang, C. K. C. Lock, J. Quinn, Y. S. Li, D. Tian and F. Jona, *Phys. Rev. B* **38**, 5363 (1988).

³M. Wuttig, Y. Gauthier, and S. Blügel, *Phys. Rev. Lett.* **70**, 3619 (1993).

⁴M. Wuttig, C. C. Knight, T. Flores, and Y. Gauthier, *Surf. Sci.* **292**, 189 (1993).

⁵W. L. O'Brien, J. Zhang, and B. P. Tonner, *J. Phys.: Condens. Matter* **5**, L515 (1993).

⁶W. L. O'Brien and B. P. Tonner, *Phys. Rev. B* **51**, 617 (1995).

⁷J. A. Martín-Gago, R. Fasel, J. Hayoz, R. G. Agostino, D. Naumovic', P. Aebi, and L. Schlapbach, *Phys. Rev. B* **55**, 12 896 (1997).

⁸A. P. Graham, B. J. Hinch, G. P. Kochanski, E. M. McCash, and W. Allison, *Phys. Rev. B* **50**, 15 304 (1994).

⁹A. P. Graham, W. Allison, and E. M. McCash, *Surf. Sci.* **269**, 394 (1992).

¹⁰A. Biedermann, O. Genser, W. Hebenstreit, M. Schmid, J. Redinger, R. Podloucky, and P. Varga, *Phys. Rev. Lett.* **76**, 4179 (1996); A. Biedermann, M. Schmid, and P. Varga, *Phys. Rev. B* **50**, 17 518 (1994).

¹¹R. Toomest, A. Theobald, R. Lindsay, T. Geißel, O. Schaff, R. Didszhun, D. P. Woodruff, A. M. Bradshaw, and V. Fritzsche, *J. Phys.: Condens. Matter* **8**, 10 231 (1996).

¹²A. Abrami *et al.*, *Rev. Sci. Instrum.* **66**, 1618 (1995); B. Brena, G. Comelli, L. Ursella, and G. Paolucci, *Surf. Sci.* **375**, 150 (1997).

¹³M. A. Van Hove and S. Y. Tong, *Surface Crystallography by Low Energy Electron Diffraction* (Springer, Berlin, 1979).

¹⁴J. Cerdá, F. J. Palomares, and F. Soria, *Phys. Rev. Lett.* **75**, 665 (1995).

¹⁵J. Cerdá, Ph.D. Thesis, Universidad Autónoma de Madrid, 1995.

¹⁶W. H. Press, S. A. Teulosky, W. T. Wetterling, and B. P. Flannery, *Numerical Recipes* (Cambridge University Press, New York, 1992).

¹⁷G. Kleinle, W. Moritz, D. L. Adams, and G. Ertl, *Surf. Sci.* **219**, L637 (1989).

¹⁸G. Kleinle, W. Moritz, and G. Ertl, *Surf. Sci.* **238**, 119 (1990).

¹⁹J. B. Pendry, *J. Phys. C* **13**, 937 (1980).

²⁰C. Polop, C. Rojas, E. Roman, J. A. Martín-Gago, B. Brena, D. Cocco, and G. Paolucci (unpublished).

²¹R. Fasel and J. Osterwalder, *Surf. Sci. Lett.* **2**, 359 (1995).

²²A. Locatelli, B. Brena, G. Comelli, S. Lizzit, G. Paolucci, and R. Rosei, *Phys. Rev. B* **54**, 2839 (1996).

²³R. Gunnella, E. L. Bullock, L. Patthey, T. Abukawa, S. Kono, C. R. Natoli, and L. S. O. Johansson (unpublished).

²⁴E. L. Bullock, R. Gunnella, L. Patthey, T. Abukawa, S. Kono, C. R. Natoli, and L. S. O. Johansson, *Phys. Rev. Lett.* **74**, 2571 (1995).

²⁵R. Gunnella, E. L. Bullock, C. R. Natoli, R. I. G. Uhrberg, and L. S. O. Johansson, *Surf. Sci.* **352-354**, 332 (1996).

²⁶C. S. Fadley, M. A. Van Hove, Z. Hussain, and A. P. Kaduwela, *J. Electron Spectrosc. Relat. Phenom.* **75**, 273 (1995).

²⁷J. Mustre de Leon, J. J. Rehr, C. R. Natoli, C. S. Fadley, and J. Osterwalder, *Phys. Rev. B* **39**, 5632 (1989), and references therein.

²⁸B. Utter and R. A. Bartynski, *Surf. Sci. Lett.* **370**, L226 (1996).

²⁹S. Gota, R. Gunnella, Z. Y. Wu, G. Jezequel, C. R. Natoli, D. Sebilliau, E. L. Bullock, F. Proix, C. Guillot, and A. Quemerais, *Phys. Rev. Lett.* **71**, 3387 (1993).

³⁰J. Zegenhagen, E. Fontes, F. Grey, and J. R. Patel, *Phys. Rev. B* **46**, 1860 (1992).

³¹D. L. Adams, H. B. Nielsen, and J. N. Andersen, *Surf. Sci.* **128**, 294 (1983).

³²C. Polop, J. L. Sacedón, and J. A. Martín-Gago, *Surf. Sci.* (to be published).

³³J. A. Martín-Gago, R. Fasel, J. Hayoz, R. G. Agostino, D. Naumovic', P. Aebi, and L. Schlapbach (unpublished).